SURFACE ENHANCED RAMAN SPECTROSCOPY APPLICATION FOR ART MATERIALS IDENTIFICATION

Elena Shabunya-Klyachkovskaya[1*], Olga Kulakovich[1], Svetlana Vaschenko[2], Dmitry Guzatov[3] and Sergey Gaponenko[1]

[1]*National Academy of Sciences of Belarus, B.I. Stepanov Institute of Physics, Nezavisimosti Avenue 68, 220072 Minsk, Belarus*
[2]*Belorussian State University, Nezavisimosti Avenue 4, Minsk 220030 Belarus*
[3]*Yanka Kupala Grodno State University, Ozheshko 22, Grodno 230023, Belarus*

Abstract

The using of plasmon Au films atop the inorganic pigments surfaces provide a huge enhancement (10^5-10^7 times) of Raman scattering. The technique of sample preparation proposed has been applied for the inorganic art pigment identification in several works of art. The masses of the fragments under investigation were not bigger than 1 µg. Obtained Surface Enhanced Raman spectra are characterized with significant signal/noise ratio while the Raman spectra in the absence of gold nanoparticles have not been recorded at all. So, the presented ultrasensitive technique could be successfully applied in the daily practice of cultural heritage study.

Keywords: nanoparticles, ultramarine blue, malachite, azurite, cerulean blue

1. Introduction

The identification of inorganic art materials in the icons or paintings provides valuable information that could be used for their study, ascription and conservation. The inorganic pigments are metals oxides, hydroxides and salts. So, they could be differed from each other by their chemical composition. Nowadays X-ray fluorescent and laser induced breakdown spectroscopy are the most widely used methods for qualitative elemental composition study of works of art in museums laboratories. It should be noted, there are some pigments that are characterized with the same elemental composition but have different chemical structure and possess other physical properties. To distinguish such pigments molecular spectroscopic techniques should be applied.

Raman spectroscopy is one of the most effective techniques of substances identification owing to the fact that the frequency set of the Raman spectrum is determined by the structure of the substance under investigation. However,

---

[*]E-mail: e.sh-k@imaph.bas-net.by, phone: +375172806264

Raman scattering has very low yield and therefore it needs large amount of material to be examined. Additionally, since Raman scattering is rather weak it is readily masked by uncontrollable intrinsic fluorescence of the analysed probe. That is why Raman spectroscopy has a very limited application in the cultural heritage study.

The Surface-Enhanced Raman Scattering (SERS) effect significantly enhances the scattering probability when the analyte is spatially confined within the electromagnetic field generated upon excitation of the Localized Surface Plasmon Resonance (LSPR) in a nanotexturized surface of a noble metal [1]. There is a number of techniques of synthesis and growing nanotexturized substrates with the SERS-active properties [2-5].

Recently, a number of papers have reported successful application of SERS to identify organic art materials [6-8]. However, there is some challenge to apply this technique for inorganic pigments study mainly because of the relatively large particle size of these pigments.

In our previous works [9-11] we noted the systematic enhancement of Raman scattering of micrometer sized inorganic crystallites using substrates based on colloidal Ag nanoparticles and Ag- or Au-coated Ge/Si-nanostructures.

The aim of this work is the optimization of SERS technique (the using substrates and the methods of sample preparation) on the model samples of blue and green art pigments as well as approbation of optimized technique for art pigment identification in the works of cultural heritage.

2. Theoretical calculations

Raman scattering enhancement factor has been calculated for molecular analytes using both incident intensity enhancement and photon density of states enhancement factors [12, 13]. This approach has been shown to provide reasoning to single molecule detection by means of Raman spectroscopy, which has been earlier reported [14] but remained unexplained for more than a decade. In the model, Raman scattering cross-section enhancement factor $G = \sigma/\sigma_0$ for a point-like probe located near a spherical nanoparticle σ versus Raman scattering cross-section without nanoparticle σ_0 has been calculated as a function of probe–particle distance. Calculations were made for normal orientation of the induced dipole moment under the assumption that excitation wavenumber, emission wavenumber, and plasmon resonance wavenumber coincide. Thus, calculations present ultimate enhancement of Raman scattering by spherical particles whereas the real enhancement should be definitely lower. The nanoparticles diameters were set to be 15, 60 and 100 nm. Dielectric function for silver and gold has been taken from Johnson and Christy [15]. The probe polarizability was equal to 20 Å^3.

The results of calculations are presented in Figure 1. One can see that the maximal enhancement provided by silver and gold nanoparticles occurs at a physically reasonable distance of about 2-2.5 Å because of the core polarization

effect [16] and exceeds ten and five orders of magnitude, respectively. However, enhancement decays rapidly with particle–probe distance r_{eff}. The smaller diameter of the nanoparticle the more rapidly enhancement decays. Detuning from exact plasmon resonance and difference in emission and absorption photon energy will result in lower enhancement, whereas the general distance dependence of enhancement remains similar.
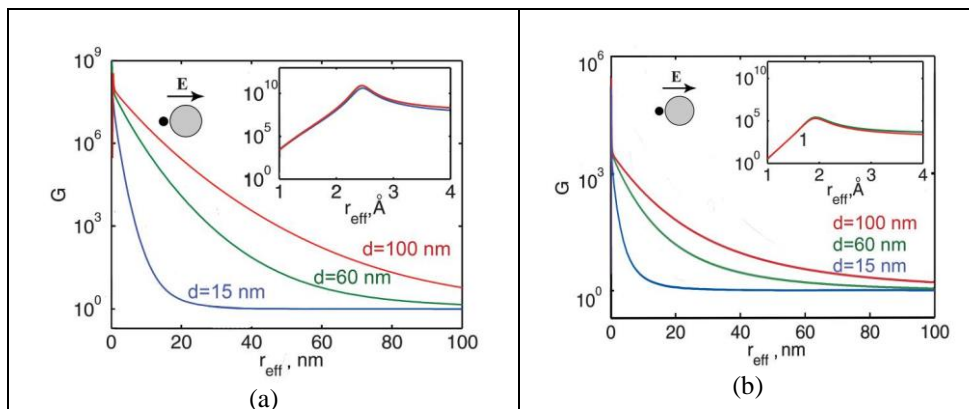
Figure 1. Calculated Raman scattering enhancement factor G versus distance r_{eff} between a point-like probe and the surface of: (a) silver and (b) gold particles with the diameter 15 nm, 60 nm and 100 nm for normal orientation of the induced dipole moment of a probe. The insets show G (r_{eff}) dependences in the close vicinity of the nanoparticles up to 4 Å.

3. Experimental

3.1. Model samples preparation

Several blue and green inorganic art pigments have been chosen as the analytes for model samples preparation. The water suspensions of the pigments have been prepared in the following concentrations (Table 1).

Table 1. Description of model pigment samples.

Pigment	Chemical formula	Producer	No.	Conc. (mol/l)	Crystallites size (μm)
Ultramarine blue	$Al_6Na_8O_{24}S_3Si_6$		#45010	$0.35 \cdot 10^{-3}$	1.25
Cerulean blue	$CoO \cdot SnO_2$	Kremer pigments (Germany)	#45730	$1.35 \cdot 10^{-3}$	1.00
Cobalt green	CoNiTiZn		#44100	$1.44 \cdot 10^{-3}$	0.75
Chrome green	Cr_2O_3		#44250	$2.11 \cdot 10^{-3}$	0.95
Malachite	$CuCO_3 \cdot Cu(OH)_2$		#10300	$1.43 \cdot 10^{-3}$	0.80

Two Ag sols with the different sizes of Ag nanoparticles as well as Au sol have been prepared to compare the nanoparticle's nature and their size influence

on the intensity in SERS spectra. The sol #Ag1 with the average nanoparticles size 15±5 nm has been prepared via $AgNO_3$ borohydride reduction [17]. Optical density spectrum of the obtained sol is characterized with the maximum on 400 nm (Figure 2a, blue line). The sol #Ag2 with the average nanoparticles size 60±10 nm has been prepared via $AgNO_3$ citrate reduction [17]. Optical density spectrum of the obtained sol is characterized with the maximum on 415 nm (Figure 2a, red line).
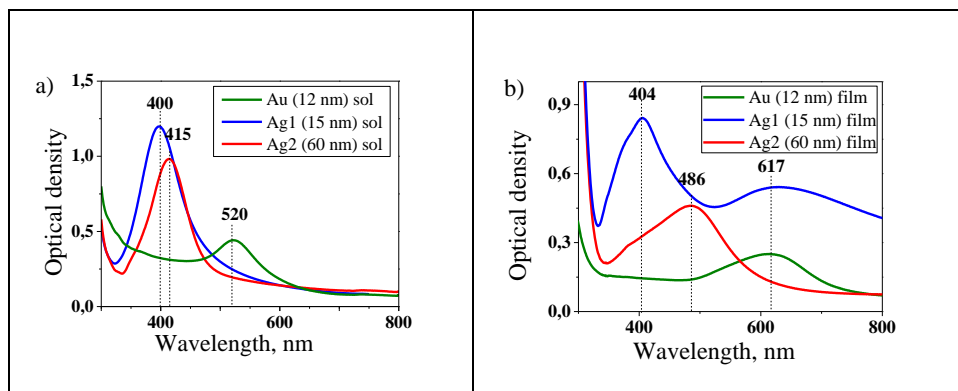
Figure 2. Optical density spectra of the: (a) gold and silver sols and (b) SERS-active substrates prepared on their bases.

.

SERS-active substrates have been prepared via layer-by-layer electostatical deposition. For this purpose glass substrates of 1×2 cm^2 in size were cleaned by means of ultrasonic treatment in isopropyl alcohol and then kept in a mixture of H_2O-H_2O_2-NH_3 (1:1:1) at 70º C for 15 min. After washing in water, substrates were covered with a polycation layer (PDADMAC, 1 g/L in 0.5M NaCl) during 20 min to develop a positive charge on a glass surface. Due to silver and gold particles were negatively charged they were deposited on PDADMAC-modified substrates by dipping the substrate surface in Ag sol for 24 h.

According to the optical density spectra of the prepared SERS-active substrates the extinction peaks of Au and Ag plasmons becomes broader and shift to the long wave region as the result of nanoparticles aggregation during the process of the immobilization. Also aggregation led to appearance of long wave extinction at 617 nm in optical density spectrum of #Ag1 film (Figure 2b, blue line).

We assumed the intensity of the peaks in SERS spectra can depend on the mutual disposition of the analytes and metal nanoparticles. That is why two ways of sample preparation have been used. In the first way 3 μl of pigment suspension was deposited *on the SERS-active substrates* and dried in the horizontal position at the room temperature. In the second way 3 μl of water suspension of the art pigments were deposited immediately *on the glass surfaces* and dried in the horizontal position at the room temperature. Then 3 μl of the sol with the metal nanoparticles was dripped atop pigments and also dried. To

compare the efficiency of the proposed techniques the reference samples of pigments in the same concentration and volume were deposited on the pure glass. So, the seven series of the model samples (Table 2) have been prepared for the experiment. It should be noted, the used concentrations of the model samples corresponded to a few µg of the pigments deposited on the substrates.

Table 2. The list of the model samples.

	Ultramarine blue	Cerulean blue	Cobalt green	Chrome green	Malachite
Series 1	Deposited on the Ag-film, prepared on the base of sol #Ag1 (15±5 nm)				
Series 2	Deposited on the glass under the drop of sol #Ag1 (15±5 nm)				
Series 3	Deposited on the Ag-film, prepared on the base of sol #Ag2 (60±10 nm)				
Series 4	Deposited on the glass under the drop of sol #Ag2 (60±10 nm)				
Series 5	Deposited on the Au-film, prepared on the base of Au-sol (12±2 nm)				
Series 6	Deposited on the glass under the drop of Au-sol (12±2 nm)				
Series 7	Deposited on the pure glass				

3.2. Experimental setup

The Raman measurements were performed in the backscattering configuration at the room temperature. The Nd:LSB laser (531 nm) has been used for Raman spectra excitation. The registration system consists of a spectrograph with a diffraction grating 1200 lines/mm (Solar TII S3801) and a cooled CCD matrix (Princeton instruments).

4. Results and discussion

4.1. Optimization of SERS technique

In the case of study chrome green and malachite Raman spectra have not been detected at all. In Raman spectra of ultramarine blue, cerulean blue and cobalt green pigments only the most intensive peaks at the 549, 667 and 729 cm^{-1}, respectively, have been detected on the essential luminescence background (Figure 3). The using of SERS-active nanostructures provides the enhancement of the peaks intensity in the spectra and the decreasing of the luminescence background simultaneously.

There is no strong dependence on the nanoparticles sizes (compare series 1, 2 with series 3, 4) and mutual analyte-nanoparticle disposition (compare series 1, 3, 5 with 2, 4, 6 respectively). In all experimental data the using of Au-based nanostructures provide the higher signal-to-noise ratio (Table 3) in comparison with the results obtained with the using of Ag-based one. It should be noted, the using of Ag-based nanostructures provides the enhancement not only chromophores peaks but the C-C bands at the 1375-1600 cm^{-1} caused by the presence of organic components (sodium citrate, polycations PDADMAC) in the sample. At the same time these bands didn't appear in the SERS spectra in the case of using Au-based nanostructures. It could be explained with the help of

215

provided theoretical calculations for molecular analytes (Figure 1) where one can see that enhancement factors (EF) provided by Ag nanoparticle are on five order of magnitude higher than EF provided by Au nanoparticle.
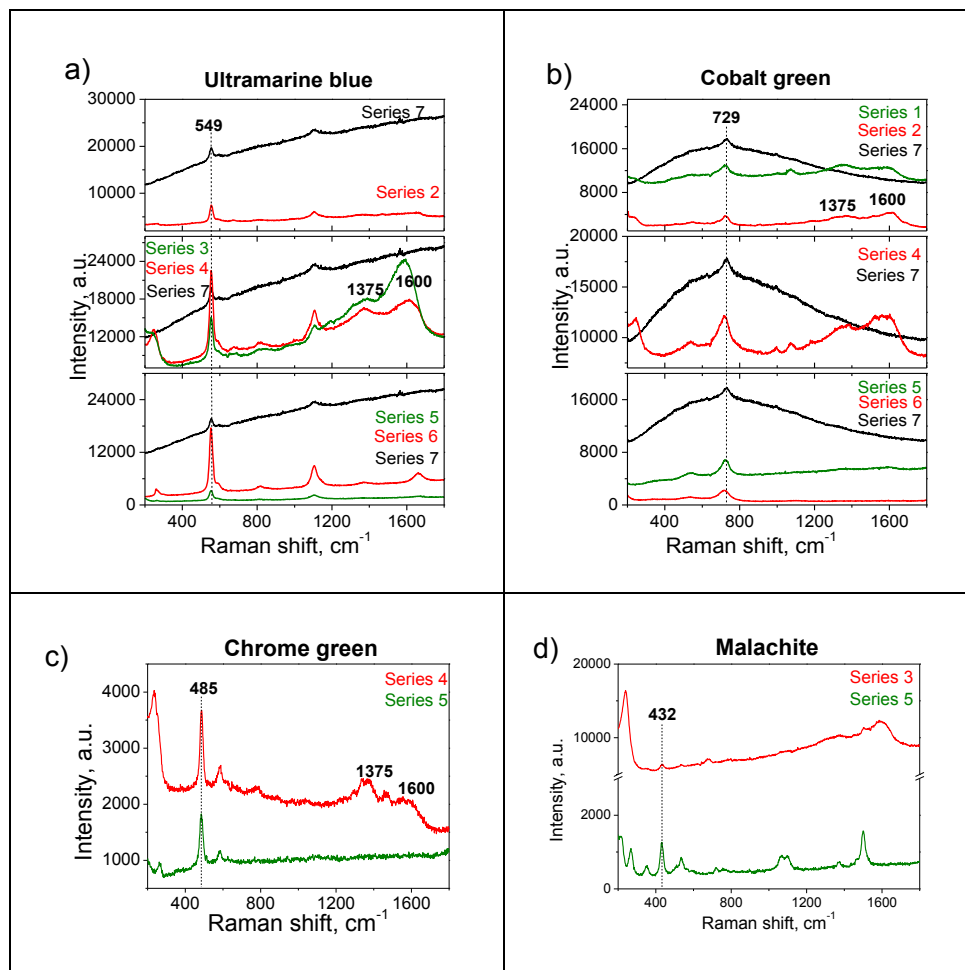
Figure 3. Raman (Series 7) and SERS (Series 1-6) spectra of: (a) ultramarine blue, (b) cobalt green, (c) chrome green and (d) malachite inorganic microcrystals.

Since the pigment crystallites sizes (0.75-1.25 μm) are too large in comparison with metal nanoparticles the huge enhancement of Raman signal is provided only in small volume of microcrystals in the close vicinity of local surface plasmon resonance (LSPR) area while the normal Raman scattering is provided by the whole volume of pigments microcrystals. So, SERS enhancement factor G can be represented as:

$$G = \frac{I_{SERS}/C_{SERS}}{I_{RS}/C_{RS}} = \frac{I_{SERS}}{I_{RS}} \cdot \frac{C_{RS}}{C_{SERS}}$$

(1)

Table 3. Signal-to-noise ratio of the most intensive peaks in the SERS spectra of art pigments.

	Malachite (432 cm⁻¹)		Chrome green (485 cm⁻¹)		Cobalt green (729 cm⁻¹)		Cerulean blue (667 cm⁻¹)		Ultramarine blue (549 cm⁻¹)	
	EF	Signal-to-noise ratio	EF	Signal-to-noise ratio	EF	Signal-to-noise ratio	EF	Signal-to-noise ratio	EF	Signal-to-noise ratio
Series 1	–	not detected	at least $1.3 \cdot 10^6$	5.2:1	$4.5 \cdot 10^5$	20.2:1	–	not detected	–	not detected
Series 2	–	not detected	–	not detected	$2.0 \cdot 10^5$	10.5:1	$2.1 \cdot 10^5$	4.2:1	$5.6 \cdot 10^6$	89.8:1
Series 3	at least $2.7 \cdot 10^4$	4.7:1	–	not detected	–	not detected	–	not detected	$3.8 \cdot 10^4$	20.6:1
Series 4	at least $1.3 \cdot 10^5$	20.3:1	at least $1.9 \cdot 10^5$	18.5:1	$1.5 \cdot 10^4$	16.7:1	$7.0 \cdot 10^3$	3.8:1	$2.8 \cdot 10^5$	118.5:1
Series 5	at least $3.6 \cdot 10^6$	19.9:1	at least $4.9 \cdot 10^6$	16.5:1	$7.7 \cdot 10^5$	29.0:1	$8.0 \cdot 10^5$	9.8:1	$1.8 \cdot 10^6$	31.0:1
Series 6	at least $1.8 \cdot 10^6$	10.3:1	at least $2.8 \cdot 10^6$	9.6:1	$6.4 \cdot 10^5$	24.5:1	$6.5 \cdot 10^5$	8.3:1	$1.2 \cdot 10^7$	177.2:1
Series 7		not detected		not detected		5.2:1		3.6:1		9.9:1

were G is the enhancement factor, I_{SERS} is the peak intensity in SERS spectrum, I_{RS} is the peak intensity in Raman scattering spectrum, C_{SERS} is the quantity of the chromophore atoms of the pigment contributed to enhanced Raman signal and C_{RS} is the quantity of chromophore atoms of the pigment contributed to original Raman signal without noble nanoparticles applied. Because the number of atoms in every crystallite is proportional to its volume it is possible to consider volume ratio V_{RS}/V_{SERS} instead of C_{RS}/C_{SERS}. Volume ratios V_{RS}/V_{SERS} for each case have been estimated on the base of theoretical calculations (Figure 1) According to the calculations the minimal distance (r_{eff}) where the

enhancement can appear is 20.5 nm for Ag nanoparticle of 15 nm in size, 57.5 nm for Ag nanoparticle of 60 nm in size and 20 nm for Au nanoparticle of 12 nm in size.

The enhancement factors (EF) estimated for each sample have been presented in the Table 3. As one can see local EF has the highest values in the case of using Au-base SERS-active nanostructures. This theoretical estimation is in good agreement with experimental data obtained. As it was mentioned above there is no strong dependence on the mutual analyte-nanoparticle disposition. So, both deposition pigment suspension on the Au-film and dripping Au sol atop of the pigment provide efficient enhancement and could be apply in cultural heritage studies.

4.2. Application of optimized SERS technique for the pigments identification

The microfragments of paints have been safely taken from the Belarusian icons 'Guiding Virgin' of the XVIIth and XVIIIth century and used in the experiment as the analytes. On the base of optimization results the monodisperse (12±2 nm) sol of gold nanoparticles has been chosen for the experiments.

According to our theoretical calculations performed for silver and gold nanoparticles (Figure 1) SERS enhancement factor achieve its maximal value when analyte is placed in the close vicinity to the silver nanoparticle and recently decay with the increasing of the distance between them.

In the reality artists paints represent themselves the multiphase system of binding media and pigment microcrystals. To provide close interaction between pigment microcrystals and gold nanoparticles binding media have been dissolved in alcohol and chloroform solutions under the slight heating and centrifuged during the 2 minutes. Chloroform suspension of the analyte pigments were deposited immediately on the glass surfaces and dried in the horizontal position at the room temperature. Then Au-sol was dripped atop the samples and also dried. Obtained SERS spectra of paints under the studying are presented in the Figure 4.

It should be noted the masses of the fragments for investigation were not bigger than 1 µg. In the same time the signal-to-noise ratio in the obtained SERS spectra is better than 25:1 while the Raman spectra in the absence of gold nanoparticles have not been recorded at all.

Spectra interpretation has been performed with the using of the base of art pigment Raman spectra [18]. So, a lot of narrow peaks are observed in the SERS spectrum of blue paint taken from the icon 'Guiding Virgin' of the XVIIIth century (Figure 4a). The peak at 406 cm^{-1} and some peaks in the region 800-1000 cm^{-1} could be ascribed to the azurite ($2CuCO_3 \cdot Cu(OH)_2$). The other peaks belong to the organic dye indigo.

In the SERS spectrum of blue paint taken from the canvas painting 'Guiding Virgin' of the XVIIth century the peaks of ultramarine blue ($Na_8[Al_6Si_6O_{24}]S_n$) appeared at 235, 563 and 1102 cm^{-1}. Malachite green

pigment ($CuCO3 \cdot Cu(OH)_2$) has been also identified by the peaks at 333, 410, 498, 645 and 1045 cm^{-1} (Figure 4b).
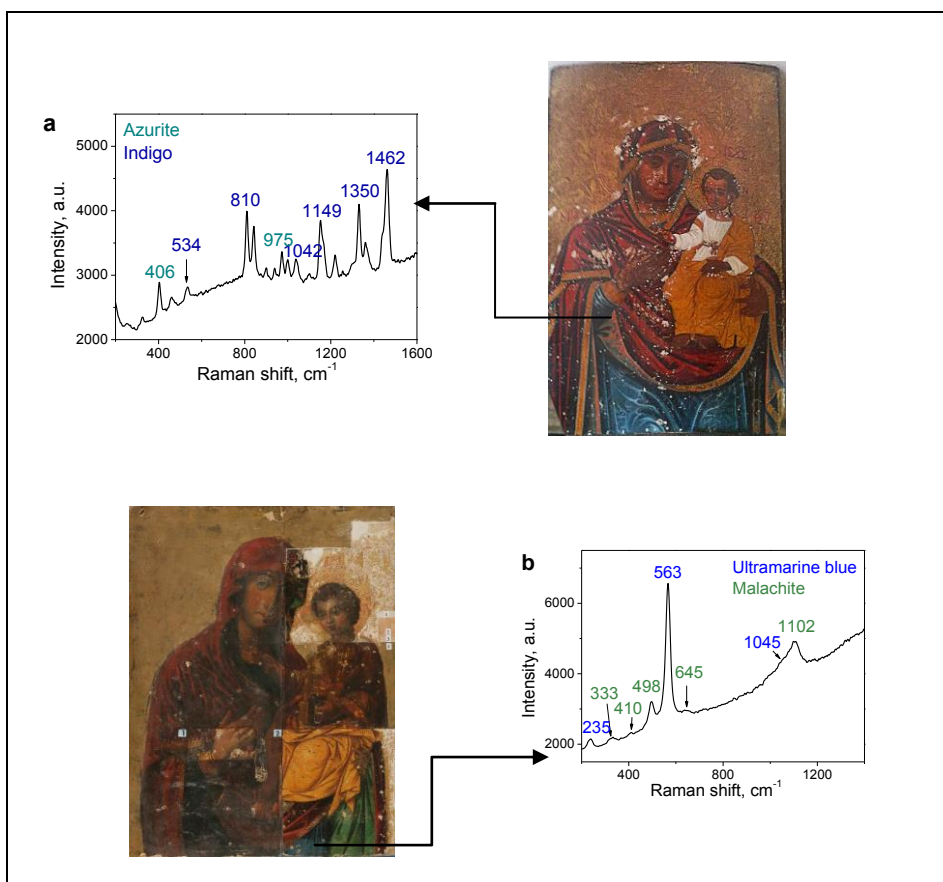
Figure 4. SERS spectra of paints taken from Belarusian icon 'Guiding Virgin': (a) of the XVIIIth century and (b) of the XVIIth century.

5. Conclusions

Some blue and green art pigments have been used as the model samples for the optimization SERS technique. The using of SERS-active nanostructures provides the enhancement of the peaks intensity in the spectra and the decreasing of the luminescence background simultaneously. There is no strong dependence of SERS intensity on the nanoparticles sizes and mutual analyte-nanoparticle disposition but in all cases the using of Au-based nanostructures provide the higher signal-to-noise ratio in comparison with the results obtained with the using of Ag-based one. The obtained experimental results are in a good agreement with the theoretical estimations of the enhancement factor. That is why Au sol has been used for pigment identification in the Belorussian icons of the XVIIth and XVIIIth century.

The signal-to-noise ratio in the obtained SERS spectra is better than 25:1 while the Raman spectra in the absence of gold nanoparticles have not been recorded at all. Ultramarine blue and malachite have been identified in the blue paint layer of the icon 'Guiding Virgin' of the XVIIth century and the azurite and indigo have been identified in the blue paint layer of the icon 'Guiding Virgin' of the XVIIIth century. So, we can conclude the presented way of sample preparation for Surface enhanced Raman spectroscopy provides huge SERS enhancement and could be successfully applied as the ultrasensitive technique in the daily practice of Cultural heritage study.

Acknowledgement

References

[1] C.L. Haynes and R.P. Van Duyne, J. Phys. Chem. B, **105** (2001) 5599.
[2] F.C. Cabrera, P.H.B. Aoki, R.F. Aroca, C.J.L. Constantino, D.S. dos Santosb and A.E. Joba, J. Raman Spectrosc., **43** (2012) 474.
[3] M.V. Chursanova, V.M. Dzhagan, V.O. Yukhymchuk, O.S. Lytvyn, M.Y. Valakh, I.A. Khodasevich, D. Lehmann, D.R.T. Zahn, C. Waurisch and S.G. Hickey, Nanoscale Res. Lett., **5** (2010) 403.
[4] E.N. Esenturk and A.R. HightWalker, J. Raman Spectrosc., **40** (2009) 86.
[5] G.M. Herrera, A.C. Padilla and S.P. Hernandez-Rivera, Nanomaterials **3** (2013) 158.
[6] I. Geiman, M. Leonaand J.R. Lombardi, Technical note, **4** (2009) 947.
[7] K.Chen, M. Leona and T. Vo-Dinh, Sensor Rev., **2** (2007) 109.
[8] S. Bruni, V. Guglielmi and F. Pozzi, Raman spectroscopy, **42** (2011) 1267.
[9] E.V. Klyachkovskaya, D.V. Guzatov, N.D. Strekal, S.V. Vaschenko, A.N. Harbachova, M.V. Belkov, S.V. Gaponenko, J. Raman Spectrosc., **43** (2012) 741.
[10] E. Klyachkovskaya, N. Strekal, I. Motevich, S. Vaschenko, A. Harbachova, M.Belkov, S. Gaponenko, C. Dais, H. Sigg, T. Stoica and D. Grützmacher, Plasmonics, **6** (2011) 413.
[11] E.V. Shabunya-Klyachkovskaya, S.V. Gaponenko, S.V. Vaschenko, V.V. Stankevich, N.P. Stepina and A.S. Matsukovich, J. Appl. Spectrosc., **81** (2014) 399.
[12] S.V. Gaponenko and D.V. Guzatov, Chem. Phys. Lett., **477** (2009) 411.
[13] S.V. Gaponenko, *Introduction to Nanophotonics*, Cambridge University Press, Cambridge, 2010.
[14] K. Kneipp, H. Kneipp, I. Itzkan, R.R. Dasari and M.S. Feld, Chem. Rev., **99** (1999) 2957.
[15] P.B. Johnson and R.W. Christy, Phys. Rev. B, **6** (1972) 4370.
[16] G.W. Ford and W.H. Weber, Phys. Rep., **113** (1984) 195.
[17] P.C. Lee and D. Meisel, J. Phys. Chem., **86** (1982) 3391.
[18] I.M. Bell, R.J.H. Clark and P.J. Gibbs, Spectrochim. Acta A, **53** (1997) 2159.